Coupled Analysis of Deepwater Oil Offloading Buoy and Experimental Verification

Sangsoo Ryu, Arun S. Duggal, Caspar N. Heyl, Yonghui Liu
FMC SOFEC Floating Systems, Inc.
Houston, TX 77040, USA

ABSTRACT

Deepwater offloading buoys have a relatively small displacement when compared to other floating systems, with the majority of the displacement being used to support its mooring system and the oil offloading lines. This results in a floating system that has a very active response to the environment coupled with feedback from the mooring and flowline systems.

Comparison of experimental data and coupled analysis results shows that viscous modeling of the buoy skirt by applying a Morison drag force formulation based on relative velocity can be used to better predict the pitch motion. As the operating water depth increases, prediction of full 6 degree-of-freedom (DOF) motions of the offloading buoy becomes more difficult since the mass/damping/stiffness contribution of mooring system and oil offloading lines becomes even more influential than that of the buoy. Thus, the coupling between mooring lines/oil offloading lines and the buoy hull becomes more complex.

Both time- and frequency-domain approaches were applied to predict the vertical plane motions, i.e. surge, heave, and pitch, of the deepwater buoy. It is found that the pitch motion is sensitive to the drag effect of the skirt, and is coupled with both surge and heave motions, and that a time-domain fully coupled analysis can capture the viscous drag effect. Results from two experiments, one with a freely floating buoy and the other with a moored buoy, are presented to show that the proposed time-domain coupled analysis predicts the buoy motion behavior very well for both cases.

KEY WORDS: Deepwater oil offloading buoy; coupled analysis; floating body dynamics; mooring analysis; Morison equation

INTRODUCTION

Deepwater offloading buoys are being extensively used in West Africa to allow efficient loading of spread-moored FPSOs. Some of the current projects of the offloading buoys include Agbami (Nigeria, 1435m water depth), Akpo (Nigeria, 1285m), Bonga (Nigeria, 1000m), Dalia (Angola, 1341m), Erha (Nigeria, 1190m), Girassol (Angola, 1320m), Greater Plutonio (Angola, 1310m), and Kizomba A & B (Angola, 1200m, 1000m). Compared to other floating systems such as TLP, spar, and FPSO, deepwater offloading buoy systems are relatively unique as mass, damping, and stiffness of the mooring lines and oil offloading lines (OOLs) are considerable compared to the inertia, radiation damping, and hydrostatic stiffness of the buoy. The motion behavior of this system has been shown to result in severe fatigue damage to the mooring and flowline components, and thus must be estimated accurately to ensure that the system is designed with sufficient fatigue life.

In a deepwater buoy system it is necessary to identify and implement the effect of both inertia and viscous loadings on each object of the buoy system since the fundamental natural periods of the buoy are in the range of first order wave loading, and the system is sensitive to damping. To accurately capture the viscous effect, a fully-coupled time-domain analysis and a diffraction model of the buoy with viscous drag elements are employed.

The objective of the paper is to show the development of a numerical model to better predict the motions of the buoy coupled with the mooring lines. Results from time- and frequency-domain calculations of the offloading buoy system are presented. The results are also compared to results from model tests of a freely floating buoy and a moored buoy to demonstrate the accuracy of the computational methods being employed to predict the buoy motions. The results and comparisons demonstrate the importance of accounting for the viscous modeling of a buoy skirt. Results from sensitivity studies are also presented to show the importance of the contribution of a skirt in prediction of motion response amplitude operators (RAOs).

MATHEMATICAL FORMULATION

To consider coupling and interactions between a buoy and mooring lines, the following differential equation is considered.

$$\{M + M_a(\infty)\}\ddot{\vec{X}} + \int_0^\infty R(t-\tau)\dot{\vec{X}}d\tau + K\vec{X} = \vec{F}_D + \vec{F}_w^{(1)} + \vec{F}_w^{(2)} + \vec{F}_{line} \quad (1)$$

where M and M_a represent the mass and added mass matrices, R the retardation function matrix, K the hydrostatic stiffness matrix, $\vec{X}$ the body displacement, $\vec{F}_D$ the drag force, $\vec{F}_w^{(1)}$ and $\vec{F}_w^{(2)}$ the first- and second-order wave loads, $\vec{F}_{line}$ the interface loads from the mooring lines and the OOLs, and the arrow above each variable the column vector.

The drag damping in pitch/roll is known as a driving parameter in buoy responses. Consequently, for drag force calculations it is more physically reasonable to apply the relative velocity (buoy and water particles) than to use the absolute buoy velocity since the buoy velocity has similar order of values to that of surrounded water particles. Due to the moment arm effect the pitch/roll response is significantly affected by the drag force caused by the skirt especially in the range of pitch natural period. The heave response around the natural period is also controlled by the skirt drag/viscous effect.

To take into account a moving buoy in waves the following Morison force formula is applied:

$$dF = C_m A_I \ddot{\xi} - C_a A_I \ddot{x} + C_d A_D \left|\dot{\xi} - \dot{x}\right|\left(\dot{\xi} - \dot{x}\right) \quad (2)$$

where dots (·) represent the time derivatives, dF force per unit length, C_m inertia coefficient, C_a added inertia coefficient, C_d drag coefficient, $A_I = \rho\pi D^2/4$, $A_D = \rho D/2$ (for a cylinder), ξ water particle displacement, and x buoy displacement.

DESCRIPTION OF MODEL TEST

The model test program was specifically designed to study the deepwater buoy at a large scale. Due to the large typical prototype depth (greater than 1,000m) and the limitation of the basin facility the decision was made to model the buoy and the environment at a large model scale. The mooring system was represented by a simplified anchor leg system that resulted in similar stiffness and natural periods as a prototype buoy in 1,000 meters of water.

Two sets of model tests were performed: (1) a freely floating buoy (very soft springs used) and (2) a moored one. The freely floating tests were designed to provide data for the response of the buoy with no mooring influence to allow direct validation of the buoy hull model response. The second set of tests was performed with a simplified mooring system to provide data for the response of the buoy influenced by the mooring system. Model tests were conducted in the Offshore Engineering Basin at the Institute for Marine Dynamics in Canada.

Model Basin

The tank is 75m long by 32m wide with a variable water depth of up to 3m as shown in Figure 1. The wavemakers consist of 168 rectangular panels across the front of the tank and along the side in an "L" formation.

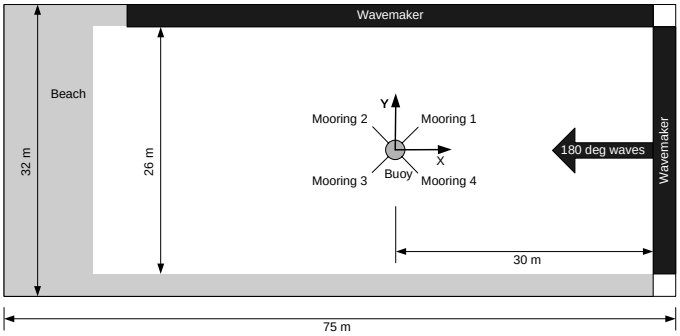

Fig.1 Plan view of the experimental configuration of deepwater buoy.

Model

The buoy hull for the test is modeled at a scale of 1:35.6. For the first set of tests in a horizontal mooring system the buoy was ballasted to have a free-floating draft of 5.65 meters. For the second set of tests the pretension of the mooring system resulted in a draft of 5.65m. The model is fitted with a skirt which has 18 holes. Mooring lines were terminated at load cells to measure the mooring tension at the skirt. All instrument cables were routed out of the buoy model through a suspended umbilical cable as shown in Figure 2. The buoy particulars for both cases are listed in Table 1.

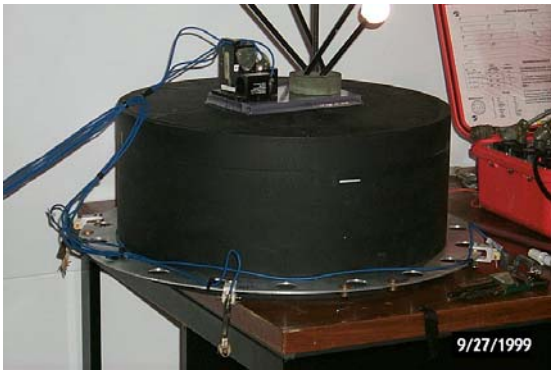

Fig.2 Deepwater buoy model.

Table 1. Buoy model particulars.

	Unit	Mooring 1	Mooring 2
Model Test Scale		35.6	35.6
Water Depth	m	106.8	106.8*
Buoy Hull Diameter	m	17.0	17.0
Skirt Diameter	m	21.0	21.0
Buoy Height	m	7.65	7.65
Draft	m	5.65	5.65
Weight in Air	ton	1293.2	878.6
KG	m	3.84	3.40
Buoy Total Rxx	m	3.82	4.39
Buoy Total Ryy	m	3.82	4.39
Fairlead Radius	m	9.50	9.50
No. of Mooring Legs		4	4

(* Note that the equivalent water depth for mooring 2 is 1,000m.)

Mooring Configurations

The first mooring configuration was designed to investigate the motions of a freely floating buoy with minimal influence of the

mooring system. The horizontal mooring system consisted of a 4 lines with soft springs that maintained the buoy at the desired location but had minimal feedback to the wave frequency motions. The second mooring system configuration was designed to have the stiffness characteristics and pretension of a 1,000m mooring system for an offloading buoy. To simplify the mooring (and its modeling) the mooring was represented by four legs spaced 90 degrees apart, with fairlead angles of 45 degrees. The pretension was designed to provide the net mooring and offloading system load on the buoy (to give the desired draft of 5.65m). The mooring system was further simplified to be as light as possible with minimal drag so that the stiffness was primary influence on the buoy response. Details of the two systems are provided in Table 2.

Table 2. Particulars of the two mooring configurations.

	Unit	Mooring 1	Mooring 2
Length	m	350	133.3
Wet Weight	kg/m	NA	3
Diameter	mm	NA	NS
EA	MT	180	1963
Pretension	MT	22	150
Fairlead Angle	deg	0	45

HYDRODYNAMIC CHARACTERISTICS & MODELING

The modeling of a deepwater buoy is complex due to the coupling between buoy, mooring and flowlines. In addition the viscous forces due to the interaction of the environment (fluid) with the hull, mooring and flowlines further complicate the analysis of the system. The objective of the current study is to focus on the accurate modeling of the fluid interaction with the buoy hull, accounting for both the inertia and viscous forces on the system.

To accurately predict the motions of the buoy, a fully coupled time-domain analysis of a buoy mooring is used since the influence of the inertia and drag of the skirt for the motions of the buoy is one of the driving factors. An appropriate modeling of the buoy skirt drag and inertia effect and the estimation/ implementation of the viscous damping of the buoy hull is addressed.

Higher-Order Boundary Element Method (HOBEM) is a state-of-the-art technique for computation of first- and second-order hydrodynamic wave forces and moments on an arbitrary three-dimensional shape body. HOBEM is used for the hydrodynamic calculations.

DeepLines, fully-coupled time-domain analysis program, is used for buoy and mooring motion analysis for both configurations. DeepLines is specifically designed for the simulation of the dynamic behaviour of flexible/rigid risers, mooring lines and umbilicals based on Finite Element modelling of slender structures.

Local Coordinate System Conventions

To conveniently describe 6-DOF buoy motions, an earth fixed coordinate system is used as shown in Figure 3. The line of wave propagation is chosen as the negative X, and Y-axis is 90 degrees counter clockwise from the X-axis. Z-axis is vertically upwards starting from the keel line of the buoy. Note that the center of gravity (CoG) of the buoy is located at (0m, 0m, 3.84m) in this local coordinate system, and all the hydrodynamic coefficients are obtained with respect to the CoG. Followed are the detailed axis conventions:

- Wave elevation positive upwards
- Surge (X-motion) along X axis
- Sway (Y-motion) positive based on a right-handed system
- Heave (Z-motion) positive upwards
- Roll positive starboard down
- Pitch positive bow down
- Yaw positive bow to portside

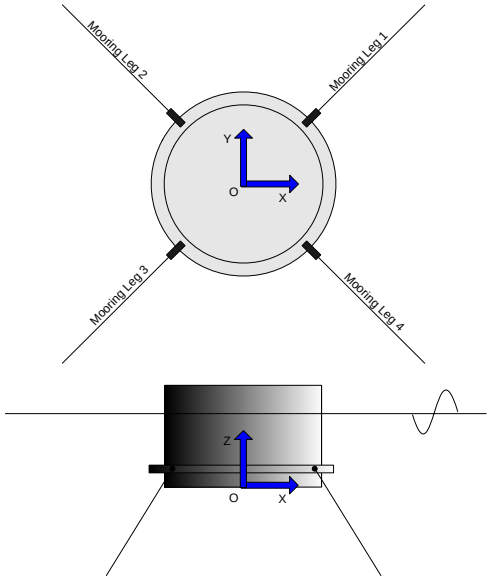

Fig.3 Buoy local coordinate system.

Hydrodynamic Calculations

HOBEM allows arbitrary higher-order variation of the potential and geometries on each isoparametric element (e.g., quadratic or cubic variation). The higher-order isoparametric elements represent the geometric body surface and potential utilizing same interpolation (or shape function) on each element. The shape functions have been well developed so that the continuity of the geometries and potential from one element to another can be assured. This HOBEM code uses 8- or 9-node quadrilateral and 6-node triangular quadratic elements. Compared with conventional panel methods, the convergence of HOBEM is considerably improved and more accurate results can be obtained with fewer boundary elements, which substantially reduce the CPU time.

Utilizing the symmetrical properties of the buoy in X- and Y-axes, a quarter of the buoy was meshed. HOBEM provides the wave exciting forces/moments, added mass and radiation damping, and hydrostatic stiffness. These hydrodynamic results are then arranged for the DeepLines calculations by properly considering phase and sign conventions of each term.

Added Mass and Radiation Damping

To take into account the skirt effect on added mass and radiation damping, the skirt is included in the mesh generation for the radiation problem. The holes on the skirt were not meshed since they were known to cause numerical instability. The viscous modeling of the skirt will be explained later in this section. Diagonal and important coupled added mass and radiation damping terms are shown in Figures 4 and 5.

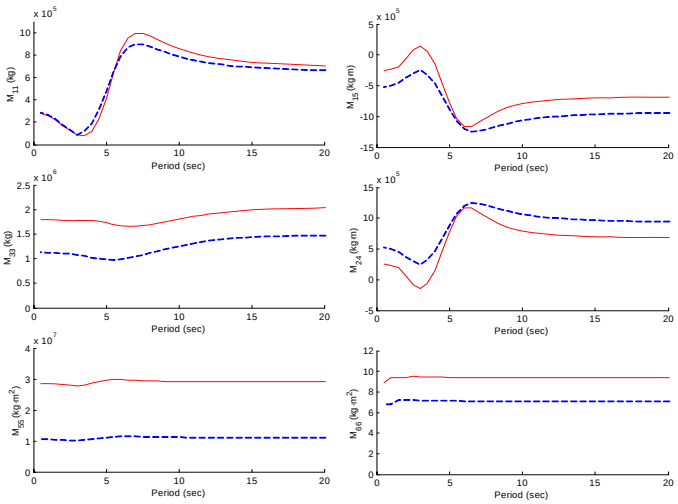

Fig.4 Added mass of the offloading buoy (solid red line – 2m width skirt included; dashed blue line – no skirt).

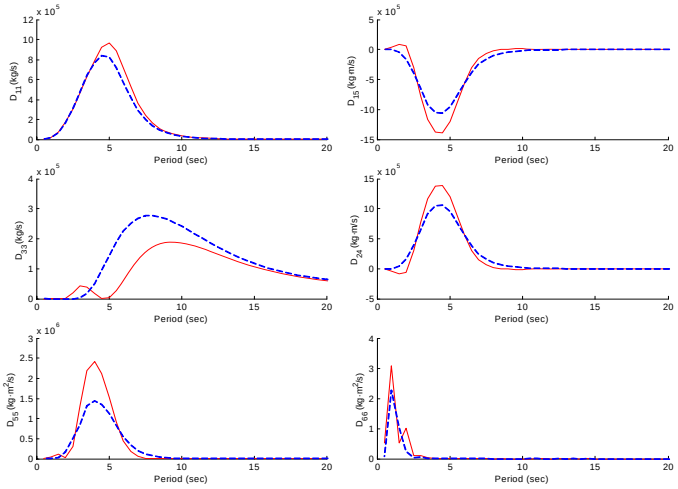

Fig.5 Radiation damping of the offloading buoy (solid red line – 2m width skirt included; dashed blue line – no skirt).

Hydrostatic Stiffness and Mass Matrices of the Buoy

The hydrostatic stiffness obtained at the CoG in the local coordinate system described above is summarized in Table 3.

Table 3. Buoy hydrostatic stiffness matrix (in N/m, N and N-m)

Mode	Surge	Sway	Heave	Roll	Pitch	Yaw
Surge	0	0	0	0	0	0
Sway	0	0	0	0	0	0
Heave	0	0	2.28e6	0	0	0
Roll	0	0	0	2.76e7	0	0
Pitch	0	0	0	0	2.76e7	0
Yaw	0	0	0	0	0	0

Wave Exciting Loads in Vertical Plane

The head wave condition and 36 wave periods from 0.5 to 22 seconds were selected, and the corresponding first order wave exciting loads in the vertical plane are shown in Figure 6.

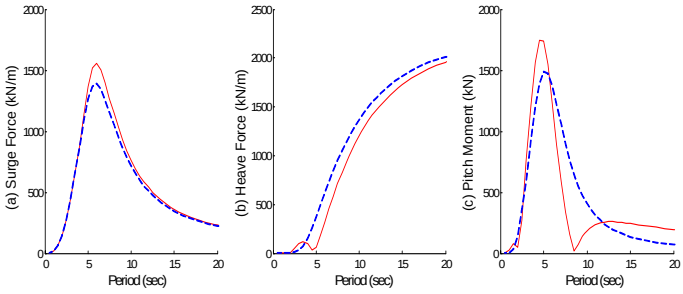

Fig.6 For the head wave condition, first order wave exciting force/moment in (a) surge, (b) heave and (c) pitch directions (solid red line – 2m width skirt included; dashed blue line – no skirt).

Mean Drift Force

Three horizontal mean drift forces and their corresponding phases are calculated and taken into account for the time-domain analyses. The surge mean drift force is shown in Figure 7.

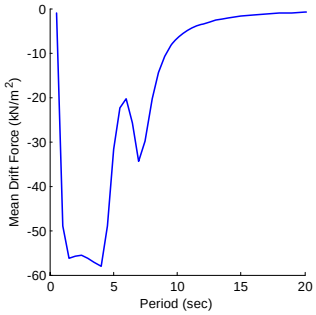

Fig.7 Surge mean drift force for 2m skirt case.

Skirt Modeling and Consideration of Viscous Damping

The method of the viscous estimation of roll/pitch is based on Valliet et al. (2002), which states that the viscous damping of the buoy with a skirt is divided into two separate damping contributions. An analytic formula, Eq. (3), for a barge is applied for the damping from a buoy hull without a skirt.

$$C = \frac{1}{2}\rho C_d B^4 L \dot{\phi}\left|\dot{\phi}\right| \tag{3}$$

where ρ is water density, C_d drag coefficient, B beam, L length, and $\dot{\phi}$ angular velocity. To apply this formula for a buoy, the definitions of parameters in Eq. (3) are shown in Figure 8.

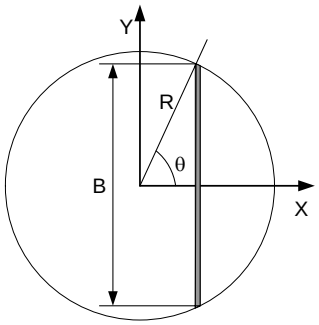

Fig.8 A schematic diagram for the mathematical derivation of roll/pitch damping.

The associated total drag roll/pitch moment is derived as follows,

$$dM_{hull} = \frac{1}{2}\rho C_d B^4 L \dot{\phi}\left|\dot{\phi}\right| \tag{4}$$

$$\begin{aligned} M_{hull} &= \int_0^{\pi} \frac{1}{2}\rho C_d \left(2R\cos\theta\right)^4 R d\theta \dot{\phi}\left|\dot{\phi}\right| \\ &= 3\pi\rho C_d R^5 \dot{\phi}\left|\dot{\phi}\right|. \end{aligned} \tag{5}$$

To take into account viscous/drag effects caused by a skirt, Morison type drag elements are implemented by using multiple disks (See Figure 9.). Viscous coefficients Cd = 0, 30, 50 are applied, and heave and pitch motions were thoroughly investigated by comparing with model test results including free-decay tests.

Not only does the buoy skirt affect the added mass and radiation damping, but it generates either viscous damping and/or drag-induced exciting force depending on its relative velocity to the wave kinematics in the surrounded velocity field since nonlinear drag force proportional to the relative velocity squared can contribute as both exciting and damping forces.

Since the skirt-induced added mass and inertia force are already taken into account in the radiation/diffraction problem, in a time-domain analysis only the viscous coefficient is included. The inertia coefficient of the disks was set to zero. The detailed viscous/drag modeling in each 6-DOF direction is summarized in Table 4.

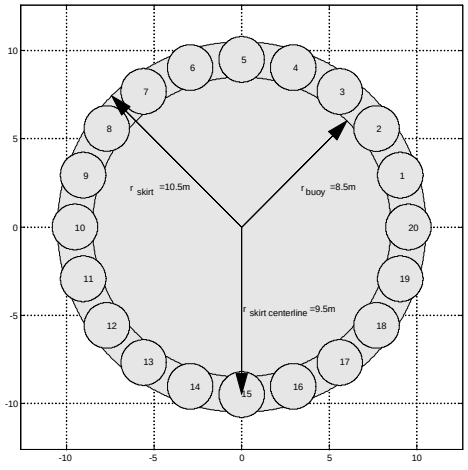

Fig.9 Skirt modeling by using multiple disks.

Table 4. Summary of buoy viscous/drag modeling.

Mode		Velocity Applied		Linear or Quadratic		Cd or D
		Absolute	Relative	Linear	Quadratic	
Surge			√		√	1.2
Sway			√		√	1.2
Heave			√		√	6.0
Roll	Hull	√			√	8.56e8
	Skirt		√		√	50.0
Pitch	Hull	√			√	8.56e8
	Skirt		√		√	50.0
Yaw		√			√	1.20e6

MODEL TESTS VS. CALCULATIONS

A series of comparisons are made between the numerical simulations and the model test results. First, a comparison is made of the free decay tests with both mooring configurations to provide a basic comparison of the numerical model and the model test data. This demonstrates the accuracy of the numerical model to capture the damping in individual modes and the natural periods. The second set of comparisons focuses on the RAOs of the buoy estimated from the model tests and the numerical simulations for both mooring configurations. The data is presented to allow comparison of both frequency- and time-domain models, and for both mooring configurations.

Free Decay Tests

Surge, heave, and pitch free decay experimental data and fully coupled time-domain calculations are compared and shown in Figures 10 through 14, for both mooring configurations. Since the surge free decay motion of the freely floating buoy is an over-damped case, only heave and pitch free decay tests are presented. Note that both the heave and pitch modes are strongly influenced by the skirt (added mass and damping) and that the numerical simulation accurately replicates the model test results. This demonstrates that the skirt model implemented in this paper is a good representation of the actual fluid-structure interaction.

Buoy Motion RAOs

Comparisons are made for both mooring configurations: (1) buoy in horizontal mooring whose stiffness is negligible (see Figures 15 - 17), and (2) simplified mooring system with stiffness characteristics of a mooring in 1,000 meters of water (see Figures 18 - 20). The motion RAOs of the buoy were derived at the buoy CoG. Figures 15 through 20 present vertical plane motion RAOs, i.e. surge, heave and pitch, of the buoy. Both regular and irregular waves were used for the tests, and both frequency- and time-domain calculations were conducted as a comparison.

Motion RAOs were extracted for both regular and irregular wave cases. The waves are incident head-on for all cases. Data obtained from the model tests and shown in the figures is extracted from six different seastates with peak periods, Tp = 4.5, 6, 8, 9, 11 and 15 seconds, respectively.

Figures 15 through 17 present the comparisons for the surge, heave and pitch RAOs for the freely floating buoy (horizontal mooring).

Figures 18 through 20 present the same information for the moored buoy (1,000m). The figures are arranged to allow direct comparison of the results from the two cases; however, note that the scale is not the same for each case. The figures compare the model test data to numerical simulations carried out in both the time- and frequency-domain. Two sets of frequency domain results are provided (a) from a diffraction analysis conducted with out modeling the skirt (freq-domain w/o skirt) and (b) from a diffraction analysis with a correction for the added mass and damping generated by the skirt.

Figure 15 presents the surge RAO for the freely floating case and shows that all three numerical models match the data well. Figure 18 presents the surge RAO for the moored buoy. Note that the surge natural period is at 19 seconds and its influence on the surge response is observed at the lower periods. Compared to Figure 15 the moored buoy has a larger surge response than the free floating buoy.

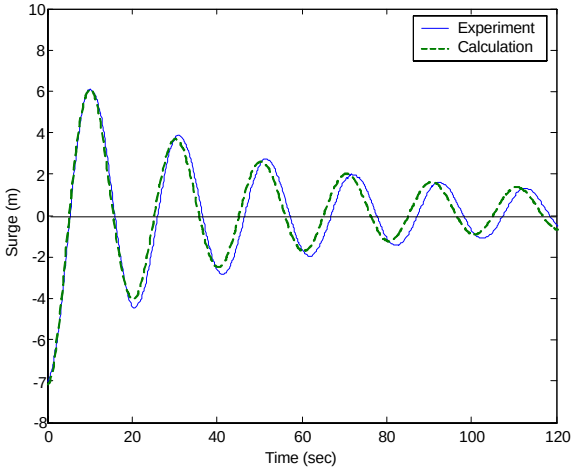

Fig.12 Surge free decay test for the moored case: solid line - experiment, dashed line – calculation.

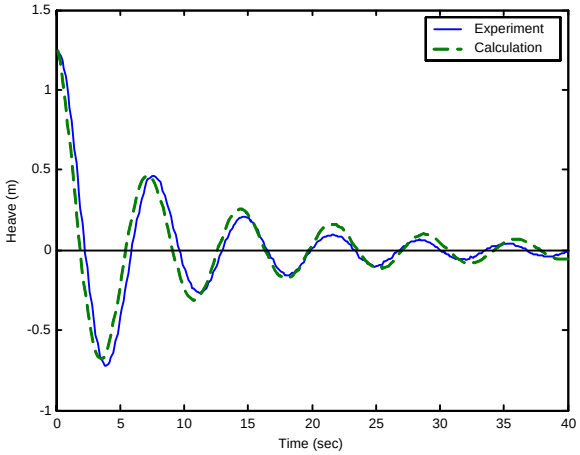

Fig.10 Heave free decay test for the freely floating case: solid line - experiment, dashed line – calculation.

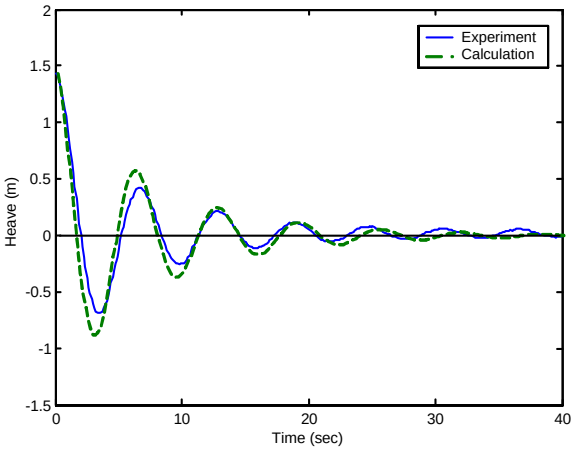

Fig.13 Heave free decay test for the moored case: solid line - experiment, dashed line - calculation.

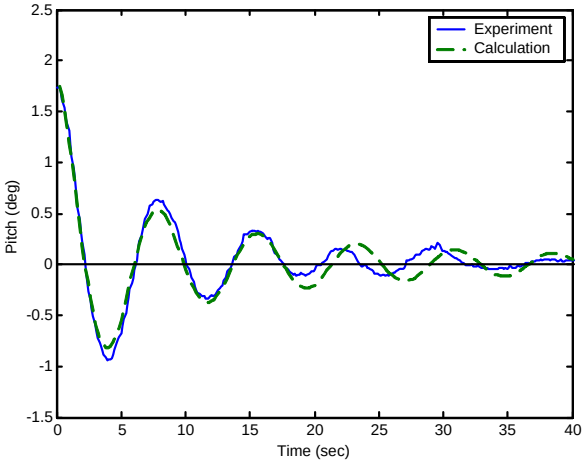

Fig.11 Pitch free decay test for the freely floating case: solid line - experiment, dashed line – calculation.

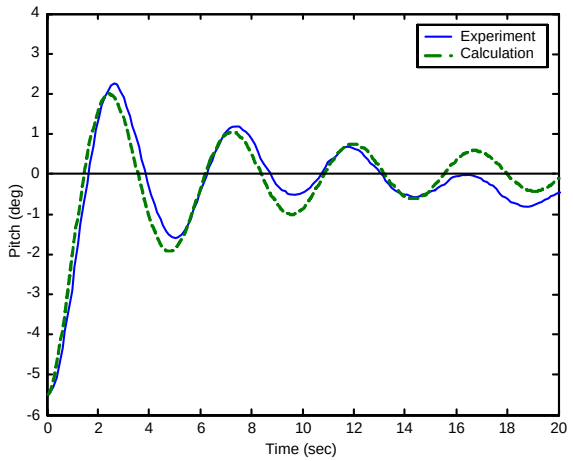

Fig.14 Pitch free decay test for the moored case: solid line - experiment, dashed line - calculation

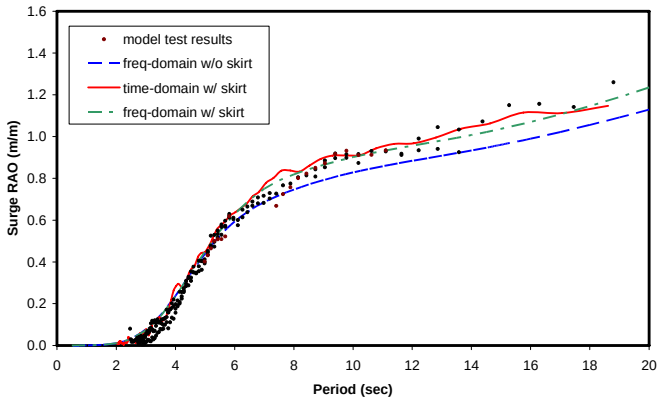

Fig.15 Surge RAOs for freely floating case: Dot – model test, blue dashed – freq-domain w/o skirt, green dashed – freq-domain w/ skirt, and red solid – time-domain w/ skirt.

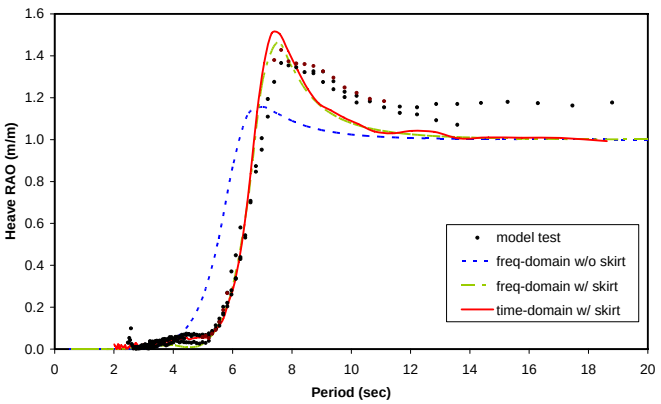

Fig.16 Heave RAOs for freely floating case: Dot – model test, blue dashed – freq-domain w/o skirt, green dashed – freq-domain w/ skirt, and red solid – time-domain w/ skirt.

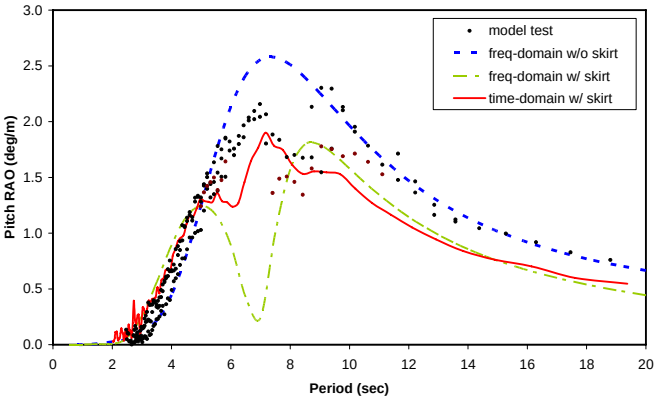

Fig.17 Pitch RAOs for freely floating case: Dot – model test, blue dashed – freq-domain w/o skirt, green dashed – freq-domain w/ skirt, and red solid – time-domain w/ skirt.

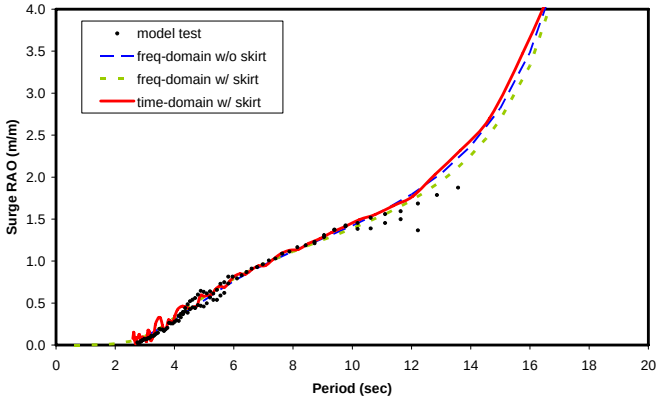

Fig.18 Surge RAOs for moored case: Dot – model test, blue dashed – freq-domain w/o skirt, green dashed – freq-domain w/ skirt, and red solid – time-domain w/ skirt.

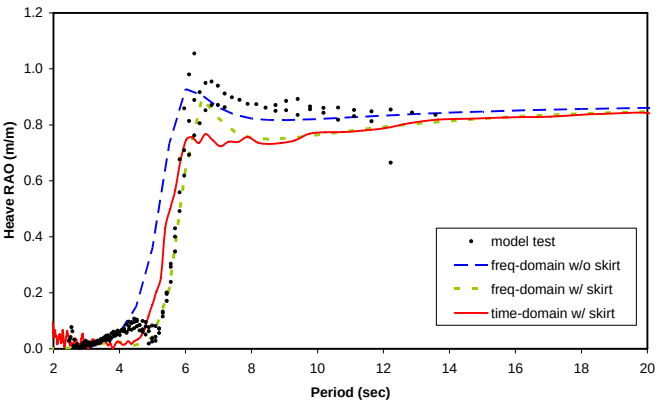

Fig.19 Heave RAOs for moored case: Dot – model test, blue dashed – freq-domain w/o skirt, green dashed – freq-domain w/ skirt, and red solid – time-domain w/ skirt.

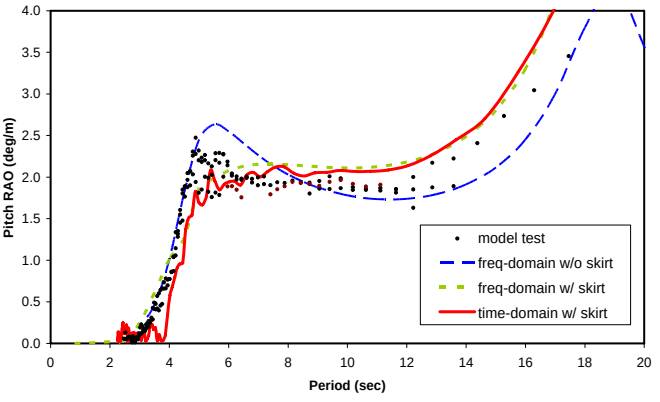

Fig.20 Pitch RAOs for moored case: Dot – model test, blue dashed – freq-domain w/o skirt, green dashed – freq-domain w/ skirt, and red solid – time-domain w/ skirt.

Figures 16 and 19 present the heave RAO of the freely floating and moored buoys, respectively. As expected the numerical model that did not account for the skirt does not match the data well. However, the numerical models with the skirt model implemented provide an adequate representation of the model test response. Note that the moored buoy has a reduced heave response compared to the free floating buoy and that the predicted response is a bit lower than that measured. Figures 17 and 20 present the pitch RAO of the freely floating and moored buoy respectively. For the free-floating buoy there is a wide range in the frequency and time domain predictions compared to the model test data.

Note that Figure 20 illustrates the coupling between surge and pitch for the moored buoy and its influence on the overall pitch response that is greater than that of the free floating buoy. This demonstrates the importance of the mooring and flowline system on the buoy response and the influence of the added mass and damping of the lines not considered here (due to the small diameter of the model test mooring lines).

CONCLUSIONS AND FUTURE WORK

This paper presents a coupled analysis of deepwater oil offloading buoy with emphasis on better buoy motion prediction with viscous modeling of the buoy skirt. Hydrodynamic characteristics of the buoy model and the skirt viscous modeling were addressed. To estimate overall damping amount of the entire system, free decay tests for surge, heave, and pitch motions were conducted.

Both frequency- and time-domain approaches were presented and compared. To validate the suggested numerical modeling, two sets of model tests, i.e. a freely floating case and a moored case, were carried out and analyzed. Based on analyzed comparisons, the following conclusions can be made:

- For the cases the skirt was not modeled in the hydrodynamic model, the corrections to the heave and pitch added-masses should be evaluated in order to obtain an accurate estimation of the heave and pitch natural periods.
- For the freely floating case the time-domain analysis with skirt viscous modeling is a better predictor of the pitch motion around the natural period than the frequency-domain analysis which has a deep valley in a pitch motion RAO due to wave exciting pitch moment cancellation resulting from the existence of a skirt in the diffraction/radiation model.
- Because of the size of a buoy the inertia effect on buoy hull can be dominant, however the viscous effect on a skirt influences heave and pitch motion responses in natural period region.
- Skirt radiation damping is negligible compared to skirt viscous damping.
- Estimating the viscous drag coefficient of the disks surrounding the buoy hull is the key to matching both heave and pitch motions of the buoy.

In this study the viscous modeling of the buoy hull was based on a quadratic form of the absolute velocity. Quantitative comparison of relative velocity based and absolute velocity based viscous modeling is a topic of future work. As the skirt viscous damping plays an important role in determining the buoy response, a more detailed study in defining the optimum damping to minimize buoy heave and pitch motions is of interest.

The paper demonstrates the sensitivity of the buoy to added mass and damping and thus the influence of the mooring and riser mass, added mass and damping will have a large effect on the deep water buoy response requiring a coupled analysis in either the frequency- or time -domain.

ACKNOWLEDGEMENTS

The authors are very grateful to Dr. D.B. Colbourne for his effort and report on experiment conducted at the IMD.

REFERENCES

Colbourne, DB (2000). "Deep Water CALM Buoy Moorings Wave Basin Model Tests," *Technical Report*, Institute for Marine Dynamics, National Research Council Canada, TR-2000-06.

Valliet, F, Cuenca, A, and Le Buhan, P (2002). "JIP CALM Buoy Model Test Results and DeepLines Calibration," *Technical Report*, Principia R.D. Ret.25.084.01.

DeepLines Theory Manual, V4.1, 2004.

Fernandes, AC, Lima ALS, and Oliveira, CAF (2003). "Frequency Domain Analysis of a Deepwater Monobuoy and Its Mooring," *Proc of OMAE 2003*, OMAE, Cancun, Mexico.

Ran, Z and Kim, MH (1997). "Nonlinear Coupled Responses of a Tethered Spar Platform in Waves," *Intl J Offshore and Polar Eng*, Vol. 7, No 2, pp 111-118.

JIP CALM Buoy Phase II Technical Report (2005). CTR1-Buoy hydrodynamics – Model tests analysis, Report No. Ret5.5.005.01.